ANNALES
UNIVERSITATIS MARIAE CURIE-SKŁODOWSKA
LUBLIN – POLONIA

VOL. LXIII, 13 SECTIO AA 2008

Investigation of surface properties of lunar regolith – Part IV♣

E. Robens[1*], A. Dąbrowski[2], E. Mendyk[2], J. Goworek[2], K. Skrzypiec[2], M. Drewniak[2], M. Dumańska-Słowik[4], W. Gac[2], R. Dobrowolski[2], S. Pasieczna-Patkowska[2], M. Huber[3], M. Iwan[2], K. J. Kurzydłowski[5], T. Płociński[5], J. Ryczkowski[2], Z. Rzączyńska[2] and J. W. Sobczak[6]

[1]Institut für Anorganische Chemie und Analytische Chemie, Johannes Gutenberg-Universität, Duesbergweg 10-14, D-55099 Mainz, Germany, erich.robens@t-online.de

[2]Maria Curie-Skłodowska University. Faculty of Chemistry, pl. Marii Curie-Skłodowskiej 2, 20-031 Lublin, Poland, dobrow@hermes.umcs.lublin.pl

[3]Maria Curie-Skłodowska University, Department of Geology and Protection of Litosphere. Institute of Earth Science, Al. Kraśnicka 2cd, 20-718 Lublin, Poland, mhuber@biotop.umcs.lublin.pl

[4] Department of Mineralogy, Petrography and Geochemistry. Faculty of Geology, Geophysics and Environmental Protection, AGH-University of Science and Technology, 30-059 Kraków, Al. Mickiewicza 30., dumanska@uci.agh.edu.pl

[5] Warsaw University of Technology. Pl. Politechniki 1, 00-661 Warszawa, Poland, tplocinskia@inmat.pw.edu.pl,

[6] Institute of Physical Chemistry. Polish Academy of Sciences. Kasprzaka 44/52, PL-01-224 Warszawa, Poland, jws@ichf.edu.pl

We investigated three lunar regolith powder samples from the Apollo missions. Apollo 11 and Apollo 12 samples come from lunar maria and Apollo 16 sample from a highland region. In the present paper we summarise in brief results of measurements using photoelectron spectroscopy (XPS), micro-Raman spectroscopy (RM), x-ray diffraction (XRD), x-ray fluorescence spectroscopy (XRF), temperature programmed

♣ This paper is dedicated to professor E. Chibowski on the occasion of his 65th birthday

* Author for correspondence: erich.robens@t-online.de

reduction and oxidation (TPRO), thermogravimetry (TG), differential thermal analysis (DTA) and nitrogen adsorption. Parts of samples are visualised by means of scanning electron microscopy (SEM/EDX) and atomic force microscopy (AFM).

1. INTRODUCTION

Between 1969 and 1972 six Apollo missions brought back 382 kg of lunar rocks, core samples, pebbles, sand and dust from the lunar surface. The six space flights returned 2200 separate samples from six different explorations sites on the moon. In addition, three automated Soviet spacecraft returned samples totalling 0.300 kg from three other lunar sites. Lunar soil and rock samples of the Apollo and Luna missions have been examined in detail [1-5]. Planning of new missions and establishing of a manned station at the moon require some more information. Therefore we analysed the chemical composition and the mineralogical structure of three soil samples of different origin using new methods and modern equipment. The assumption of an inventory of water ice suggests studying the surface properties of regolith in contact with water [6]. Besides remainders of bulk ice from asteroidal impacts, water- if present at the moon - could exist as chemisorbed and vicinal water in some depth in regions, which are protected from sun irradiation. Therefore new investigation and evaluation methods have been applied for water sorption measurements at the samples [7-9]. Looking at the moon with the naked eye, it can be seen easily that there are bright and dark areas called 'maria' on its surface [10]. Telescopic observations showed that the maria are very flat, and are very different from the heavily cratered and mountainous so-called highlands. We have learned that the maria are relatively young areas on the moon which were generated after very large impacts penetrated moon's crust and excavated the basins. During later volcanic episodes, liquid magma came to the surface and filled these basins. As this happened in comparatively recent times, the number of impact craters is far less than in the highland areas.

Impact processes have formed the lunar regolith. The regolith top moon's crust varies from 3 to 5meters in the maria to 10 to 20 meters in the highlands. Lunar soil is the subcentimeter fraction (<1mm) of the lunar regolith. Detailed studies have shown that five basic particle types make up the lunar soils: mineral fragments, pristine crystalline rock fragments, breccia fragments, glasses of various kinds, and the unique lunar structured particles called agglutinates [1].

2. SAMPLES

The Apollo samples are handled and stored either under vacuum or in clean dry nitrogen gas at the Astromaterials and Curation Office of the NASA's Johnson Space Center, Houston, Texas [11]. Three samples each of about 3g were chosen from the material gathered during Apollo 11, 12 and 16 missions, respectively. The mineral and chemical composition of the lunar soils depends on the mission landing sites [12]. Apollo 11 and Apollo 12 landed well inside mare basalt regions, and consequently, soil samples from these sites have abundant mare-derived basaltic rock clasts and mafic minerals like olivine and pyroxene. On the other hand Apollo 16 landed in highland regions. Soils from this mission contain abundant highland-derived components, e.g. lithic fragments of anorthositic rocks, breccias, and anorthitic feldspar.

The measurements described in refs. [13,14] were performed with the original samples, which have been exposed to the atmosphere for transfer into the measuring equipment. The present measurements had been carried out with those samples already investigated. The surface of which may be regarded as contaminated by residuals of water molecules or organic molecules. However, our adsorption experiments reported in refs. [13,14] have shown that only few amounts of gas or vapour are adsorbed and subsequently had been desorbed in vacuum completely even at ambient temperature. So we may value the results presented here as to be authentic for the lunar material. Indeed, lunar material has found to be stable in earth's atmosphere also by other authors [2,3,5], although slow oxidation of metallic Fe grains may occur.

3. INVESTIGATIONS

The present paper provides a survey on measurements performed at Maria Curie-Skłodowska University (UMCS), Lublin, AGH-University of Science and Technology, Cracow, Warsaw University of Technology, and the Polish Academy of Sciences, Warsaw. Other investigations made at the University of Münster, Germany and at POROTEC GmbH, Hofheim, Germany have been published elsewhere [13,14]. The present report covers some results of x-ray photoelectron spectroscopy (XPS), micro-Raman spectroscopy (RM), induction coupled plasma mass spectrometry (ICP-MS), Fourier transform infrared photoacoustic spectroscopy (FTIR/PAS), x-ray diffraction (XRD), x-ray fluorescence spectroscopy (XRF), temperature programmed reduction and oxidation (TPRO), thermogravimetry (TG), differential thermal analysis (DTA) and volumetric adsorption measurements. Parts of samples are visualised by means of scanning electron microscopy (SEM/EDX) and atomic force microscopy (AFM).

4. X-RAY PHOTOELECTRON SPECTROSCOPY (XPS)

X-ray scattering techniques are a family of non-destructive analytical techniques, which reveal information about the crystallographic structure, chemical composition, and physical properties of materials and thin films. If the sample is irradiated with soft (preferably monochromatic) x- rays then the photoelectrons are emitted from the sample surface. Atomic number of the emitting element and valence of its atoms determine the energy of these photoelectrons, so that surface chemical state is obtained. These energies are typically less than 2000 eV. Since the XPS method is surface sensitive, an ultra high vacuum must be kept in a spectrometer system during analysis. If the incident energy is high enough, an electron from the near-nucleus core is set free, and a photoelectron is released. Then another higher situated electron falls into the generated hole. Sometimes, due to energy released in the XPS process, a third "Auger" electron is ejected, as well. Though the electrons interacts strongly with materials only those emitted from the uppermost few atomic layers can escape from the surface without energy loss and contribute to the peak. The remains, inelastic scattered photoelectrons contribute to the background spectra rather then to a specific peak. Electrostatic analyser determines photoelectrons with respect to its binding energy (BE), in spectroscopic or imaging mode [15-17]. From the binding energy and intensity of the photoelectron peak, the elemental identity, chemical state and quantity of an element are determined.

XPS spectra of all samples were acquired at room temperature using ESCALAB-210 spectrometer (VG Scientific, England) and non-monochromatic Al Kα ($h\nu$ = 1486.6 eV) X-ray radiation source, operated at 300 W (15 kV, 20 mA). Survey scan (0 - 1350 eV) was acquired at pass energy of a hemispherical analyzer of 75 eV, with step 0.4 eV. Detail spectra in all regions were acquired at pass energy 20 eV and step 0.1 eV. The samples were pressed into tablet form, attached to sample holder and evacuated to vacuum below 8 x 10^{-9} mbar without any further treatment. Data processing was performed using Avantage Data System (Thermo Electron). Data were smoothed; nonlinear Shirley background was subtracted. Peak synthesis by the symmetric Gaussian-Lorentzian product function, with L/G ratio 0.3 ± 0.05, were used to approximate the line shapes of the fitting components. For quantification the Scofield sensivity factors and determined transmission function of the spectrometer were used. Binding energy scale was referenced to the C1s peak of adventitious carbon at 285.00 eV. Typical XPS spectrum is shown in Figs 1a, 1b and the corresponding results of elemental analysis are collected in Table 1.

Tab. 1. Results of an elemental analysis for the Apollo 11 sample by XPS method.

Name	BE [eV]	FWHM [eV]	Atom %
Mg1s	1308.74	2.67	2.63
Na1s	1076.54	3.03	0.44
$Fe2p_{1/2}$ sat	733.09	4.7	0
$Fe2p_{1/2}$	728.3	4.49	0
$Fe2p_{1/2}$	723.93	2.5	0
$Fe2p_{3/2}$ sat	721.59	3.46	0
$Fe2p_{3/2}$ sat	718.11	4.01	0
$Fe2p_{3/2}$	714.85	4.05	2.51
$Fe2p_{3/2}$	710.82	2.97	0.46
$\Sigma =$			2.97
F1s A	692.49	3.17	0.28
F1s	689.21	2.75	0.22
$\Sigma =$			0.5
O1s C	538.1	1.98	2.26
O1s B	536.48	2.29	25.49
O1s A	535.16	2.21	19.18
O1s	533.79	2.3	7.1
$\Sigma =$			54.03
$Ti2p_{1/2}$	468.14	3.19	0
Ti2p sat	465.58	2.43	0
$Ti2p_{3/2}$	462.81	3.06	1.04
$\Sigma =$			1.04
$Ca2p_{1/2}$	355.81	3.28	0
$Ca2p_{3/2}$	352.17	2.89	3.06
$\Sigma =$			3.06
C1s E	292.88	2.22	0.95
C1s D	290.9	1.86	0.88
C1s C	289.73	1.84	1.65
C1s B	289.25	1.69	1.63
C1s A	288.43	1.79	3.28
C1s	287.23	1.8	0.94
$\Sigma =$			9.33
Al2s	123.45	3.28	0
Si2p A	106.65	2.76	18.59
Si2p	104.15	2.72	1.78
$\Sigma =$			20.37
Al2p	78.63	2.79	5.62
			5.62

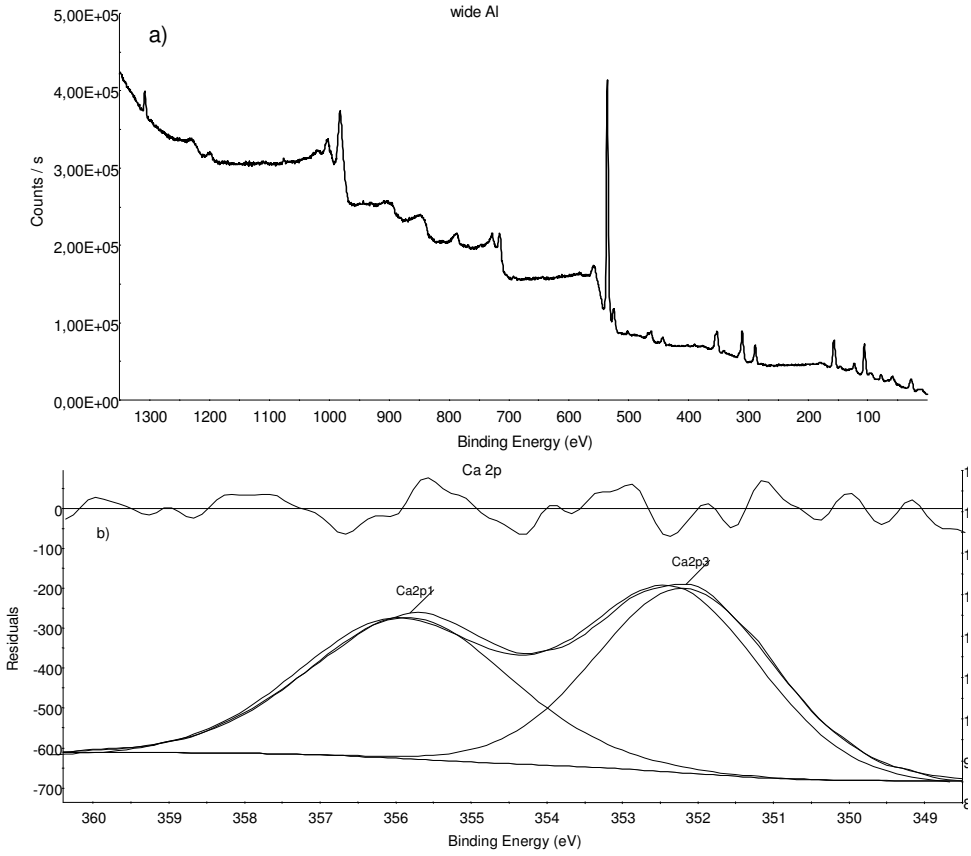

Fig 1. XPS spectrum of the Apollo 11 sample (a) and an example of the data processing for Ca bands (b).

5. X-RAY FLUORESCENCE AND X-RAY DIFFRACTION ANALYSIS

The XRF method is widely used to measure the elemental composition of materials. This method is fast and non-destructive to the sample. When an external radiation from x-ray tube or radioactive source irradiates a substance. the exciting x-ray can be absorbed by atom due to photoelectric effect. If an exciting x-ray had sufficient energy. electrons are ejected from the inner shells creating vacancies. and thus bringing the atom about an unstable state. As the atom comes back to its stable condition. electrons from the outer shells can jump in to fill the hole. Due to this process characteristic x-ray fluorescence. unique to this element is emitted with energy to be difference between the two binding energies of the corresponding shells. In the most cases K and L atomic shells are

involved in XRF detection. A typical XRF spectrum displays multiple peaks of different intensity as a function of photon energy.

An identification of elements composing the lunar samples was based on XRF method. The ED-XRF spectrometer model 1510 (Canberra Packard. USA) equipped with set of radioactive sources was used for measurements. Small samples of lunar regolith of 150 mg in size were prepared as very thin pellets with surface density of 0.0478g cm^{-2}. The excitation source was Fe-55 for light elements (from Al to Ti) or Cd-109 for heavier ones (from Ti to Mo). The mass analysis was carried out using the standardless method. The results of element abundance are given in Tables 2.

X-ray powder diffraction pattern were measured with HZG-4 Diffractometer (Carl Zeiss. Germany) using Cu Kα radiation. XRD patterns were recorded in a range of 5-95(2Θ) with step = 0.03(2Θ). For illustrative purposes XRD spectrum of the Apollo 16 sample is shown in Figure 2.

Tab. 2. XRF data. Proportions of major and trace elements in lunar soils.

Element	Apollo 11 10084.2000	Apollo 12 12001.922	Apollo 16 64501.228
Na	0.18 %	0.29 %	0.21 %
Mg	4.40 %	4.00 %	2.00 %
Al	9.51 %	9.23 %	15.13 %
Si	19.12 %	22.04 %	19.10 %
K	0.21 %	0.22 %	<787 ppm
Ca	9.85 %	8.95 %	11.84 %
Ti	5.11 %	2.12 %	0.31 %
Cr	0.21 %	0.29%	731ppm
Mn	0.14 %	0.16 %	445 ppm
Fe	10.55 %	10.91 %	2.83 %
Ni	214 ppm	137 ppm	211 ppm
Cu	-	-	36 ppm
Zn	42 ppm	-	44 ppm
Sr	138 ppm	120 ppm	149 ppm
Y	82 ppm	94 ppm	29 ppm
Zr	247 ppm	404 ppm	132 ppm
Nb	11 ppm	23 ppm	8 ppm
Pb	-	-	39 ppm

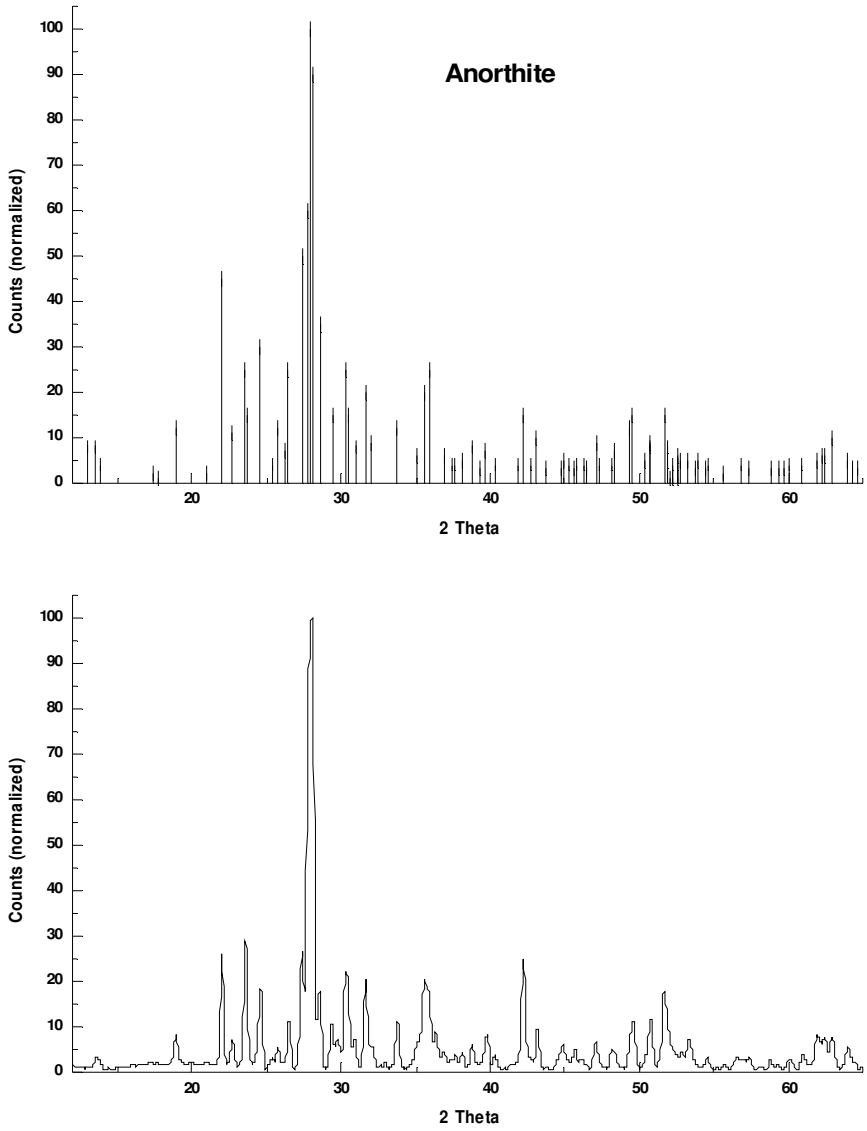

Fig. 2. Record of X-ray diffraction (XRD) of the Apollo 16 sample. The XRD diffractogram (lower picture) matches closely anorthite reference (upper library diffractogram).

6. RAMAN SPECTROSCOPY

Raman spectroscopy is a spectroscopic technique used in condensed matter physics and chemistry to study vibrational. rotational. and other low-frequency modes in a system [18]. When a laser produced monochromatic light of ultraviolet. visible or infrared frequency illuminates a sample then a very small proportion of the incident light ($\sim 10^{-6}$) is scattered at new frequencies being shifted up or down relative to the basic frequency. This wavelength difference yields the so-called Raman shift. Unchanged frequencies (due to elastic Rayleigh scattering) are filtered out and those in a certain spectral window away from the laser line are dispersed onto a detector. Raman effect can only be observed if the polarizability in molecule is changed during a normal vibration. If a phase transition occurs. the Raman spectra. which ultimately depend on crystal and molecular symmetries. will also change. Thus. Raman spectroscopy is a powerful technique for phase analysis and elucidating crystal structures. Most minerals have sharp and intensive spectral bands that allow phase identification directly from raw spectra. Because this method is non-destructive. and generally no sample preparation required. thus it is especially well suited for the study of materials like lunar samples and Martian meteorites [19-21].

The micro-Raman spectroscopy was applied in this study to identify mineralogical phases in lunar regolith. We used inVia Reflex Raman spectrometer (Renishaw plc. UK). This instrument comprises an optical microscope coupled to a single-grating spectrograph fitted with a CCD camera detector. Such coupling allows to identifying the spot of the investigated sample and making it visible by the means of false colours to distinguish between parts of different chemical composition. Raman microscope allows constructing a spectral map showing distribution of components on the analyzed surface. Precise motorized and software controlled microscopic stage make the laser spot to be placed and traveled along with a geometric grid in the X and Y directions. The two lasers of 514 or 785 nm were used for spectra acquisition and area mapping. Some examples of Raman analysis are shown in Figs 3a. b.

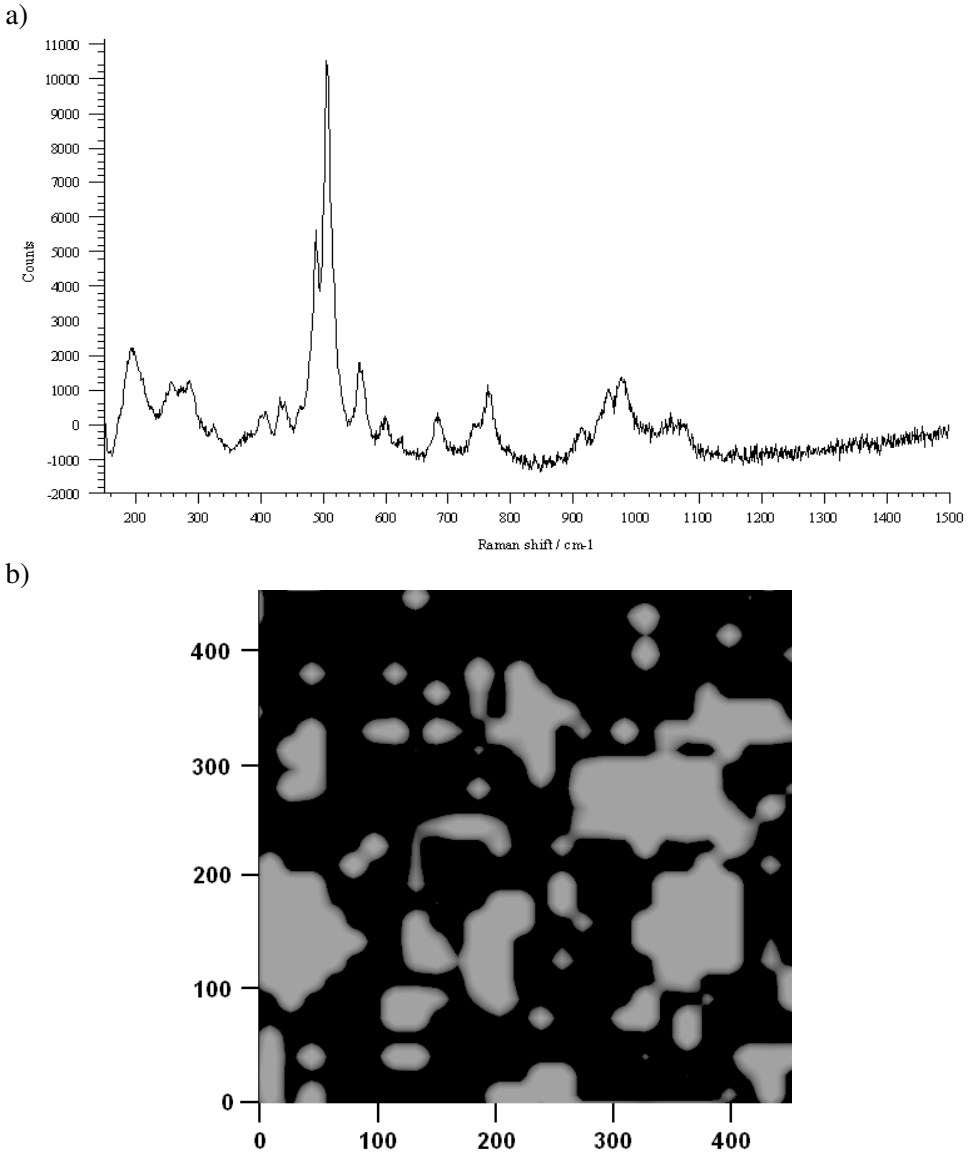

Fig. 3. Raman spectrum (a) and distribution of an anorthite (grey area) on the Apollo 16 surface sample (b). Raman image at 450 x 450 μm^2 scan size. Aquisition parameters: laser 514 nm; line focus mode: step: X = 18 μm. Y = 55.44 μm; objective: x20.

7. SCANNING ELECTRON MICROSCOPY

All three lunar samples were inspected at UMCS. Warsaw University of Technology and AGH-University of Science and Technology by means of Scanning Electron Microscopy (SEM). In a typical SEM. electrons are thermionically emitted from a tungsten or lanthanum hexaboride cathode and are accelerated towards an anode. Another types of SEM microscopes are equipped with cold field emission gun. Condenser lenses focus the electron beam into a very fine spot. The beam passes scanning coils and is deflected there horizontally and vertically so that it scans in a raster fashion over a rectangular area of the sample surface [36.37]. Secondary electrons or backscattered electrons from the sample surface are analysed. Depending on the instrument. the resolution can fall somewhere between less than 1 nm and 20 nm. X-rays. which are also produced by the interaction of electrons with the sample. may also be detected in a SEM equipped with energy-dispersive (EDX) or wavelength dispersive X-ray (WDX) probe.

Some SEM investigations were made at the AGH. Cracow. Backscattered electron (BSE) and scattered electron (SE) observations were performed using FEI Quanta 200 FEG scanning electron microscope equipped with EDS detector. The system was operated in high – vacuum mode at 15 kV accelerating voltage. In order to prevent the accumulation of electrostatic fields at the specimen during imaging the target material of Apollo 16 was sputtered with an ultra thin gold-palladium film. Such a coating improves in addition contrast and resolution but may obscure the underlying fine detail. Coating is a destructive process because it can not be removed without damaging the specimen. However. the Apollo 11 and 12 samples were analysed with carbon shadowing. The standardless method was used for elemental analysis. A typical records are shown in Figure 4a-d.

At Warsaw Technical University SEM investigation were made under low vacuum conditions. which allows for the observation of non-conducting materials without covering. The dust samples we placed on carbon foil and observed via the electron microscope (Hitachi S3500 N). A BSE detector of Robinson type was used to collect the signals from the backscattered electrons. The pictures of the dust topography were taken within the 150–2500 magnification ranges. Furthermore. energy dispersive x-ray (EDX) analysis was made using a EDS detector at a 15 kV acceleration voltage. The mass analysis was carried out using the standardless method. Some results are shown in Figure 5.

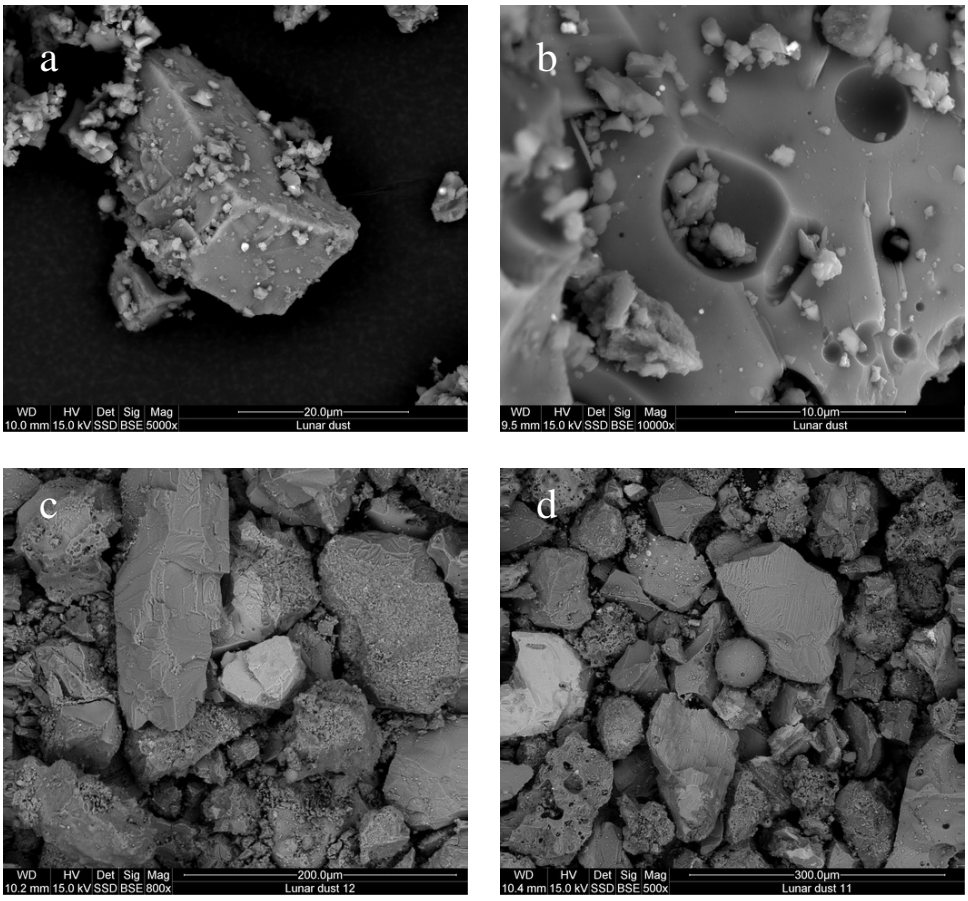

Fig. 4. SEM images of Apollo samples: Apollo16 (a. b). Apollo 12 (c) and Apollo11(d). A very small microcraters are observed on surface of the Apollo16 particle (b) and the glassy spherule of ~60 µm diameter (probably of pyroclastic origin) is seen at the centre of d micrograph (FEI Quanta 200 FEG microscope. Cracow).

8. RESULTS AND DISCUSSION OF CHEMICAL AND MINERALOGICAL ANALYSIS

The lunar regolith samples appeared as a dark grey to light grey. very fine grained. clastic. loose material primarily derived from the mechanical disintegration of anorthositing and basaltic rock. The mean grain size of analysed soils averages between 60 and 80 µm. Individual regolith particles are mostly glassy aggregates (agglutinates) and various rock and mineral fragments.

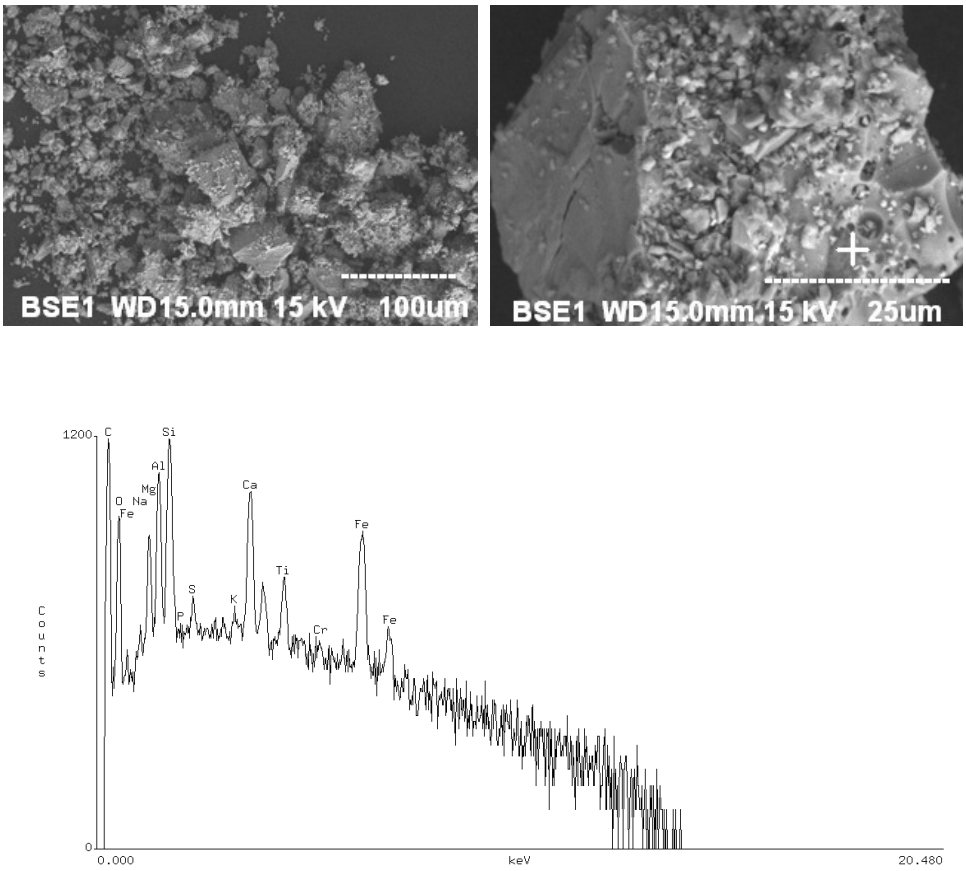

Fig. 5. SEM micrographs of the Apollo 12 sample and corresponding EDS spectrum (below) acquired from the crosshatch. (Hitachi S3500 N microscope. Warsaw).

Recent computer models indicate that the moon could have been formed from the debris resulting from the Earth being struck a glancing blow by a planetary body about the size of Mars [23-24]. We have learned that a crust formed on the Moon 4.4 billion years ago. This crust formation. the intense meteorite bombardment occurring afterward. and subsequent lava outpourings are recorded in the rocks. Radiation spewed out by the Sun since the formation of the Moon's crust. was trapped in the lunar soil as a permanent record of solar activity throughout this time [25]. Though the material covering moon's surface is similar to that of earth its history is different. On account of lacking atmosphere and water the treatment on Moon took place in a completely dry atmosphere and in a strongly reducing environment [26.27]. Thus. its mineralogical composition is relatively simple (see Table 3). Lunar rocks are divisible into three types:

basalts. anorthosites and breccias. Basalts mainly fill mare basins and anorthosites form the highlands [27.29].

Tab. 3. Minerals forming lunar rocks according to NASA [28].

	Name	Formula	Notes
Major phases	Plagioclase	$NaAlSi_3O_8 \cdot CaAl_2Si_2O_8$	almost pure anorthite $CaAlSi_2O_8$
	Pyroxene	$(Ca.Mg.Fe)_2Si_2O_6$	
	Olivine	$(Mg.Fe)_2SiO_4$	
	Ilmenite	$FeTiO_3$	
Minor phases	Iron	Fe	metallic iron grains with Co or Ni
	Troilite	FeS	only sulfide
	Silica	SiO_2	
	Chromite-ulvospinel	$FeCr_2O_4$-Fe_2TiO_4	64–65% Cr_2O_3
	Apatite	$Ca_5(PO_4)(F.Cl)$	
	Merrillite	$Ca_3(PO_4)_2$	
	Ternary feldspar	$(Ca.Na.K)AlSi_3O_8$	
	K-feldspar	$(K.Ba)AlSi_3O_8$	
	Pleonaste	$(Fe.Mg)(Al.Cr)_2O_4$	
	Zircon	ZrO_2	
	Rutile	TiO_2	
	Zirkelite-zirkonolite	$(Ca.Fe)(Zr.Y.Ti)_2O_7$	
New minerals	Armalcolite	$(Mg.Fe)(Ti.Zr)_2O_5$	70% TiO_2; pseudobrookite structure
	Tranquillityite	$Fe_8(Zr.Y)_2Ti_3Si_3O_{24}$	hexagonal
	Pyroxferroite	$CaFe_6(SiO_3)_7$	Fe-rich pyroxenoid
	Yttrobetafite	$(Ca.Y)_2(Ti.Nb)_2O_7$	unknown structure; high activity of U and Th isotopes

Plagioclase. pyroxene and olivine are the main rock minerals of the lunar surface. Plagioclase dominates in highlands. while pyroxene and olivine in mare regions. As motioned above the Apollo 11 and Apollo12 missions landed inside mare whereas the Apollo 16 landed in the highland region. Most of the Apollo 16 crystalline rock is rich in feldspar and depleted in the mafic minerals. pyroxene and olivine. The Apollo 16 regolith also contains mafic components that do not originate in the feldspathic highlands. A large proportion of the mafic material occurs as a glass. mostly of meteoroid impacts origin. The most abundant mafic material at the Apollo 16 zone is impact-melt breccia with high abundance of ITEs (incompatible trace elements such as Th) that cannot fit into a crystal structure. and thus were left behind. floating to the surface of the magma. Moreover. the concentration of Mg and Fe in this material is significantly greater in comparison to those of feldspathic lithologies. These kinds of breccias are also common among non-mare materials of all other Apollo sites. Another type of mafic material consists of products of mare volcanism. Despite the Apollo landing being 220 km from the nearest mare. small fragments of mare basalts and pyroclasic glass are founded in the Apollo16 regolith [30-

33]. The regolith of highlands is characterised by low maturity and specific Fe and Al abundance: the higher a soil maturity degree. the greater the iron and the smaller the aluminium content. This was confirmed by the data of the samples from the Apollo11. 12 and 16 missions. The Apollo basalts comprise tree class: olivine basalt. pigeonite basalt. and ilmenite basalt [34]. All basalts contain significant amounts of TiO_2. Olivine basalts are lowest in TiO_2 (2.86 to 3.0 %). pigeonite are slightly higher (3.29 to 3.38%). and ilmenite basalts have the highest level (4.8 to 5.16) [35]. In spite that Apollo 11 mission landed on Mare Tranquillitis. a few millimetres in size fragment of rocks coming from highlands were collected. These are mainly composed of plagioclase feldspar; some grains were composed exclusively of anorthositic plagioclase. The identification of this mineral rock led to bold hypothesis that a large portion of the moon was once molten. and that the crust formed by fractional crystallisation of this magma ocean. Table 4 presents the results of the chemical compositions in lunar regolith obtained by XRF spectroscopy and other analytical methods.

9. FOURIER-TRANSFORM INFRARED / PHOTOACOUSTIC MEASUREMENTS

With infrared spectroscopy a sample's absorbance is analyzed in its infrared spectrum (IR) with wavelength range of 780 – 1 nm. That absorbance spectrum is then analyzed by means of the Fourier transform method: The signal is dissolved with regard to the included frequencies and afterwards reconstructed from the frequency spectrum (FT-IR). That. in turn. allows identification of the chemical components of the sample by means of a spectrum pattern. In conventional transmission spectroscopy the measurement of absorption is transferred to a measurement of the radiation transmitted through the sample. In photoacoustic spectroscopy (PAS) the absorption radiation is determined directly via the heat released [22]. That short-time release heat produces pressure waves in the surrounding gas. hence. sound and that sound is detected by means of a microphone (FT-IR/PAS). This method is especially useful for dark and

The FT-IR/PAS were recorded by means of a Bio-Rad Excalibur 3000 MX spectrometer equipped with a photoacoustic detector MTEC 300 (with helium atmosphere in the detector) covering the 4000–400 cm^{-1} range at a resolution of 4 cm^{-1} and maximum source aperture. The spectra were normalized with reference to MTEC carbon black standard. A stainless steel cup 10-mm in diameter was filled with the dust sample (thickness < 6 mm). Before each data collection the PA cell was purged with dry helium for 5 min. Interferograms of 1024 scans were averaged for each spectrum.

Tab. 4. Chemical composition (wt. %) of basic elements in lunar regolith measured in this study in comparison to related samples of the same series [1].

Sample	Element	ED XRF	SEM / EDX*	ICP-MS	Lit. [1] p. 346
10084.2000 (Apollo 11)	Si	19.12	10.72 (13)	20.78	19.70
	Ti	5.11	0.83 (13)	2.34	4.70
	Al	9.51	2.64 (13)	2.59	7.20
	Cr	0.21	0.23 (8)	0.05	0.21
	Fe	10.55	8.76 (13)	4.16	11.9
	Mn	014	-	0.06	0.15
	Mg	-	3.44 (13)	-	4.70
	Ca	9.85	5.02 (13)	6.12	8.50
	Na	-	0.52 (8)	-	0.35
	K	0.21	-	0.05	0.13
	P	-	-	-	0.03
	S	-	0.10 (7)	-	0.12
	Ni	0.02	-	0.008	-
	Sr	0.01	-	0.01	-
	Zr	0.02	-	0.06	-
12001.922 (Apollo 12)	Si	22.04	11.18 (11)	21.53	21.60
	Ti	1.26	1.08) (10)	1.04	1.80
	Al	3.71	3.92 (11)	2.28	6.83
	Cr	0.20	0.22 (7)	0.06	0.23
	Fe	10.55	12.23 (11)	4.66	11.70
	Mn	0.16	-	0.06	0.17
	Mg	-	3.51 (11)	-	5.61
	Ca	9.85	5.16 (11)	4.91	7.65
	Na	-	0.22 (7)	-	0.40
	K	0.21	0.11 (7)	0.07	0.26
	P	-	0.12 (7)	-	0.22
	S	-	0.19 (7)	-	-
	Ni	0.01	-	0.006	-
	Sr	0.01	-	0.01	-
	Zr	0.04	-	0.009	-
64501.228 (Apollo 16)	Si	19.10	18.78.(20)	23.66	21.00
	Ti	0.31	0.46 (17)(	0.30	0.32
	Al	15.13	11.87 (20)	4.94	14.40
	Cr	0.07	0.12 (7)	0.02	0.23
	Fe	2.83	4.46 (20)	1.83	3.96
	Mn	0.04	-	0.03	0.23
	Mg	-	4.13 (18)	-	3.44
	Ca	11.84	10.81.(20) (	7.40	11.12
	Na	-	0.27 (19)	-	0.34
	K	<0. 08	0.19 (17)	0.06	0.14
	P	-	-	-	0.04
	S	-	0.16 (7)	-	0.06
	Ni	0.02	-	0.01	-
	Sr	0.01	-	0.01	-
	Zr	0.01	-	0.05	-

* Mean value. Number of measurements is shown in parenthesis.

Tab. 5. Results of FT-/PAS measurements. Wavenumbers of peaks in cm^{-1}.

Apollo 11	Apollo12	Apollo 16	Note
3432	3443	3451	ν -OH
2945	2957		ν_{as} $-CH_3$
2915	2925	2929	ν_{as} $-CH_2-$
	2857	2853	ν_s $-CH_2-$
1739			
1643	1637	1627	δ -OH
1384	1384	1385	δ_s $-CH_3$. $-CH_2-$
1046	1054	1057	
929	912	916	γ $-(CH_2)_n-$
	731	735	
	628		

From the results presented in Table 1 one can stated that small amount of water and organic hydrocarbons occur in the investigated samples. This is due to possible sample contamination during measurement of the sorption isotherms of water. heptane and octane that had already been carried out with those samples [13.14].

10. ATOMIC FORCE MICROSCOPE

All samples were investigated using an atomic force microscope (NanoScope III type. Digital Instruments. USA). a very high-resolution type of scanning probe microscope. with demonstrated resolution of fractions of a nanometer far below the resolution of SEM. The AFM consists of a microscale cantilever with a sharp tip (probe) at its end that is used to scan the specimen surface. The cantilever is typically silicon or silicon nitride with a tip radius of curvature on the order of nanometer. When the tip is brought into proximity of a sample surface. forces between the tip and the sample lead to a deflection of the cantilever according to Hooke's law. Depending on the situation. forces that are measured in AFM include mechanical contact force of different kind.

In the preceding investigation with SEM highly cleaved and porous particles had been detected [13.14]. In the present investigation single and rather smooth particles were found. AFM images reveal a rather flat and hardly structured surface without pores of nanometer scale (Figures 6a. b). This is in accordance with sorption measurements in which only few mesopores (pore width in the range of 2 to 50 nm) and no micropores (pore width below 2 nm) are indicated.

a) b)

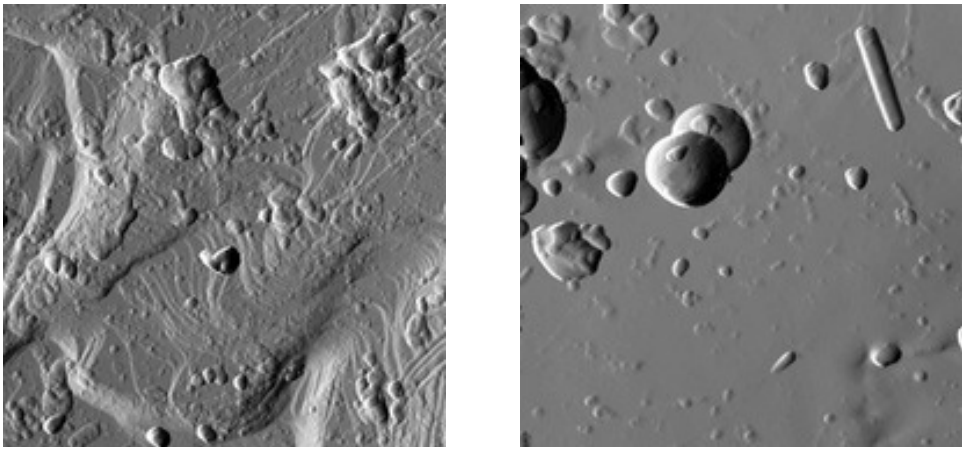

Fig. 6. Topography images of the Apollo 12 sample at 2 μm (left image) and 3 μm (right image) scan sizes. Data obtained in tapping mode in air.

11. THERMOGRAVIMETRY AND DIFFERENTIAL THERMAL ANALYSIS

Thermogravimetry TGA and Differential thermal analysis DTA studies were made in order to clear whether lunar material is able to ad- and absorb significant amounts of water and to keep water molecules. A thermogravimetric apparatus consists of a balance and a heating unit to adjust the sample temperature at a constant value or to control the defined temperature increase [38]. Measurements are made either in air. in an inert gas flow or in vacuum [39.40]. To investigate the water content measurements are performed at low temperatures. Up to 100°C physisorbed water and condensed pore water vaporise mainly. At higher temperatures chemisorbed components and crystal water are liberated.

We used a Setsys 16/18 apparatus (Setaram. France) [41]. Samples (5–8 mg) were heated at temperatures of 30–900 °C with a heating rate of 5° min^{-1} in flowing air (v =1 dm^3 h^{-1}) or argon atmosphere (v =0.8 dm^3 h^{-1}). Samples were heated in 100 μl ceramic or platinum crucibles.

We observed unexpected increase or decrease of the sample mass. respectively in ceramic crucibles at temperature above 100°C both. in air and argon atmosphere (Figure 7a, b). Obviously there was an interaction between samples and the crucible material together with the atmosphere. Literature reports [42.43] show that many metal oxides and inorganic salts (for example fluorides, ferrites of alkaline and alkaline earth metals) melt and dissolve Al_2O_3

or they form aluminates or double oxides. The TG curves obtained in air and argon atmosphere differ significantly demonstrating different reactions of the originated phase with the furnace's atmosphere.

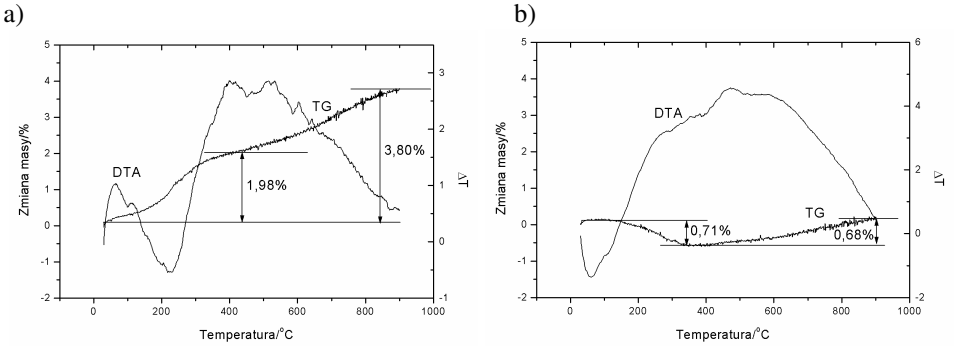

Fig. 7. TG and DTA curves of Apollo 11 sample heated in ceramic crucible in air (a) and argon(b).

Therefore we used exclusively platinum crucibles in the following experiments. Thermal analysis in argon atmosphere demonstrated that despite pretreatment by former experiments and the storage in air for some months nothing was ad- or absorbed. At temperatures up to 350 °C the TG curves remained practically on the zero level (Figure 8a). Likewise the DTA curves do not indicate any reaction without mass change. However. the sensitivity of our DTA thermocouple may be too low to reveal polymorphic transformations.

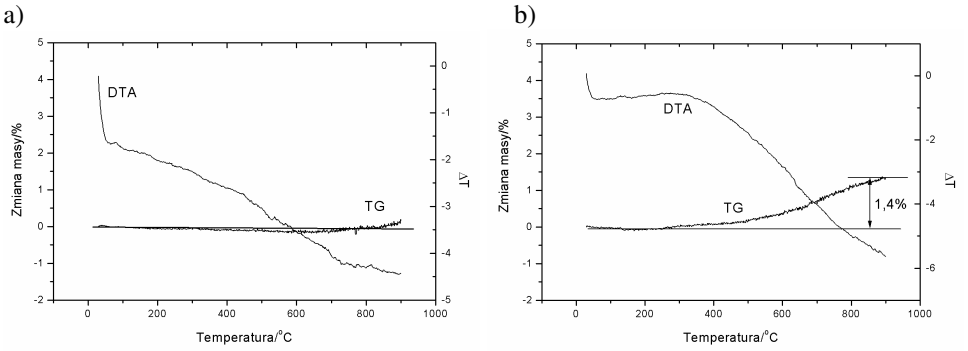

Fig. 8. TG and DTA curves of Apollo 11sample heated in platinum crucible in argon (a) and air atmosphere (b).

Above 350 °C by TG in air all lunar samples undergo slow oxidation processes (Figure 8 b). Probably oxidation of free iron present in the lunar material is oxidized or elements existing in low oxidation state are transformed to higher ones (for example Fe^{2+}. Cr^{3+}). The increase of the sample mass is connected with change of sample's color: they become brownish-red. confirming oxidation of free iron. The increases of mass are similar for Apollo 11 (1.40 %) and Apollo 12 (1.41 %) but less for the Apollo 16 sample (0.43 %). This is in accordance with the iron content of the samples (see Tables 2 and 4). Above 500 °C further increase of sample mass takes place. probably caused by oxidation of other sample components.

Results of thermal analysis show that lunar material is not hygroscopic. In contact with the atmosphere quantities adsorbed are below the detection limit of thermal analysis methods.

In order to study the interaction of lunar material with water vapor the samples were held 7 days inside of a Binder KBF 115 climatic chamber at a temperature of 85 °C and relative humidity of 95 %. At those conditions water should be physisorbed and probably chemisorbed. The high temperature required for complete dehydration is a proof of chemical bonding of water molecules. However. the quantity of bonded water is less than 1 % indicating that lunar regolith is hydrophobic.

12. TEMPERATURE PROGRAMMED REDUCTION AND OXIDATION (TPRO)

The Temperature Programmed Reduction and Oxidation is thermoanalytical technique for characterising chemical interactions between solids and reacting gases. Resulting data are commonly interpreted on a qualitative basis or by utilising simple. approximate kinetic equations. However it is possible to determine also quantity and strength of solid-oxygen. While a sample is heated at linear increasing temperature. the decomposition products or bulk species, as well as the consumption of reactive gases are monitored. Typically, a thermo-conductive detector (TCD) or a mass spectrometer is used. The heat quantity delivered to the sample induces breaking of bonds and thus the strength of interaction is closely related to the temperature of the peak generation. The surface area under the peak is related to the number of desorbed or consumed molecules. TPRO techniques have been widely used in the field of catalysis and material science for determination of the surface properties and the nature of metallic or oxidic species. To our knowledge the temperature programmed reduction-oxidation studies have not yet been applied for lunar samples.

Three samples of Apollo series were investigated in these studies. Studies were conducted on Altamira AMI-1 system (Zeton Altamira) equipped with thermal conductivity detector (TCD) and coupled with mass spectrometer HAL 211RC (Hiden Analytical). The sample (0.0500 g) was placed in the tube of 10 mm diameter. High purity He and Ar and gaseous mixtures of 6.21 % H_2 / Ar and 5 % O_2 / He were used in the experiments. Typical results are shown in Figures 9a. b.

13. SORPTOMETRY

The measurement of nitrogen adsorption isotherms at 77 K is the standard procedure to determine the specific surface are and the pore size distribution of solid surfaces [44.45]. Usually the volumetric method is applied in which the pressure decrease is measured of a determined amount of nitrogen introduced into the calibrated sample container.

Nitrogen adsorption isotherms at 77 K have been measured using a Quantachrome Autosorb-1CMS apparatus by which the volumetric method is applied. From the isotherms the specific surface area S_{BET} was calculated using the two-parameter equation of Brunauer. Emmett and Teller [46]. Furthermore the pore size distribution was established using the methods of Barrett. Joyner and Halenda (BJH) [47] and Dollimore and Heal (DH) [48] and the specific mesopores volume V_{BJH} was determined. It should be recognised that the volumetric measurement of nitrogen isotherms is at the limit of sensitivity of the instrument for such that material of low surface area which has no pores in the nanometer region. Therefore the result represented in Figure 10 and Table 6 should not be overestimated. In ref. [14] a comparison is made with results of adsorption measurements using other adsorptives.

Tab. 6. Results of the evaluation of nitrogen adsorption isotherms at 77 K.

Sample	Specific surface area S_{BET} $m^2\ g^{-1}$	Specific mesopore volume V_{BJH} cc $g^{-1}\times10^{-3}$	Specific micropore volume cc $g^{-1}\times10^{-3}$	Mean pore diameter nm
APOLLO 11 10084.2000	2.39	6.1	0	2.9
APOLLO 12 12001.922	1.77	6.3	0	3.6
APOLLO 16 64501.228	2.73	11.0	0	2.9

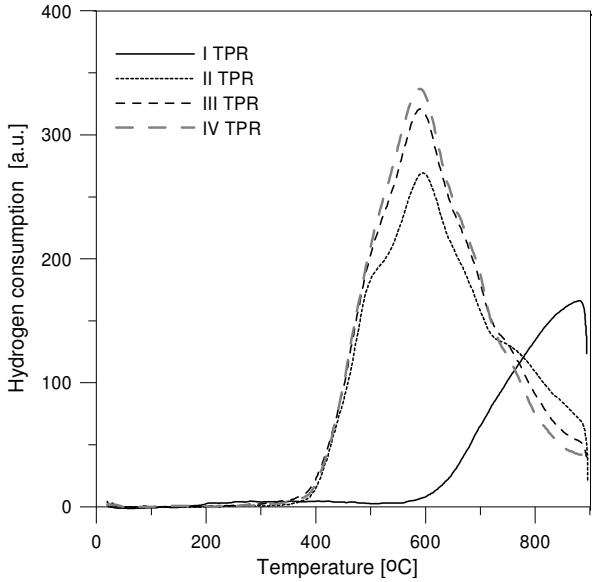

Fig. 9a. TPR curves of the A11 sample.

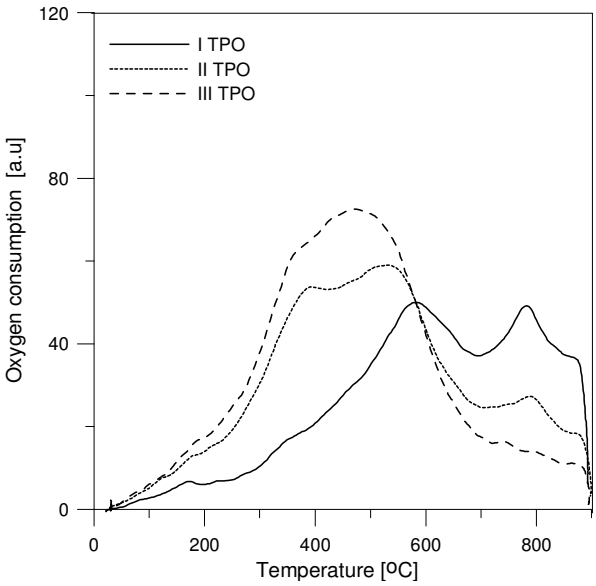

Fig. 9b. TPO curves of the A11 sample.

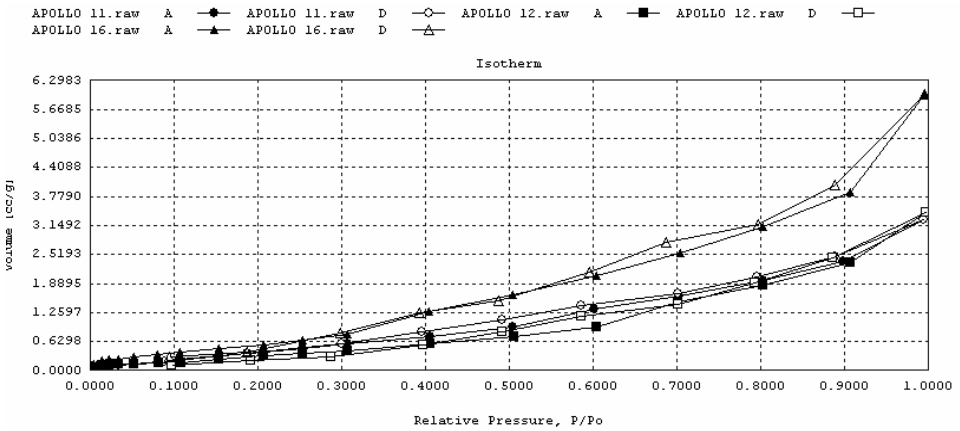

Fig. 10. Adsorption/desorption isotherms of nitrogen at 77 K for the lunar regolith samples.

14. CONCLUSIONS

Mineralogical and chemical analysis confirms results reported in the literature but the modern methods with improved resolution gave a more detailed view on composition and stracture of the samples. Sorption measurements. thermal analysis and thermogravimetry confirmed low specific surface area. low porosity and hydrophobicity of lunar regolith. So it cannot be expected that usable amounts of water be bound in the material covering moon's surface.

Acknowledgenment. The samples had been kindly placed for our disposal by the NASA Lunar sample curator. Dr. Gary Lofgren. Houston. Texas.

15. REFERENCES

[1] G. H. Heiken, D. T. Vaniman, and B. M. French, eds., *Lunar Sourcebook*, 1991, Cambridge University Press, Cambridge.

[2] D. A. Cadenhead, et al. *Some surface characteristics and gas interactions of Apollo 14 fines and rock fragments*. in *Proceedings of the Third Lunar Science Conference (Supplement 3. Geochimica et Cosmochimica Acta).* M.I.T. Press. p. 2243-2257. 1972.

[3] D. A. Cadenhead,. and R. S. Mikhail, *Water vapour weathering of Taurus-Littrow orange soil: A pore-structure analysis*. in *Proceedings of the 6th Lunar Science Conference.* p. 3317-3331, 1975.

[4] R. B. Gammage and H. F. Holmes, *Blocking of the water-lunar fines reaction by air and water concentration effects*, in *Proceedings of the 6th Lunar Science Conference,* p. 3305-3316, 1975.

[5] H. F. Holmes and R. B. Gammage, *Interaction of gases with lunar materials: Revised results for Apollo 11*, in *Proceedings of the 6th Lunar Science Conference,* p. 3343-3350, 1975.

[6] E. L. Fuller Jr. and P. A. Agron, *Sorption by low area materials*. in *Progress in Vacuum Microbalance Techniques*, C. Eyraud and M. Escoubes, Editors, Heyden: London, p. 71–82, 1975.
[7] P. Staszczuk, D. Sternik and G. W. Chadzynski, *J. Therm. Anal. Cal.* 71(1): p. 173–182 (2003).
[8] D. Sternik et al. *J. Therm. Anal. Cal.* 8 (2006).
[9] V. V. Kutarov, E. Robens and B. Kats, *J. Therm. Anal. Cal*. (2006).
[10] J. L. Josset and B. H. Foing, 2006: SPACE-X Space Exploration Institute and ESA SMART-1 Project.
[11] J. Allton, *25 Years of curating Moon rocks. http://www-curator.jsc.nasa.gov/lunar/lnews/lnjul94/hist25.htm*, 1994.
[12] D. Stöffler. A. Bischoff. et al.. *J. Geophys. Res.*. 1985(90): p. C449–C506.
[13] E. Robens et al. *Appl. Surface Sci*. 253, p. 5709–5714 (2007).
[14] E. Robens et al. *Journal of Thermal Analysis and Calorimetry* (2008).
[15] Kratos Analytical. www.kratos.com
[16] J. Wolton and N. Firley, *J. Interface Anal*. 38, p. 1230
[17] J. Wolton and N. Firley, *J. Electron. Spectrosc. relat. Phenom.* 150, pp. 15 (2006).
[18] D. J. Gardiner, *Practical Raman spectroscopy*, Heidelberg: Springer 1989.
[19] A. Wang et al. *J. Geophys. Res.* 100, pp. 21189–21199 (1995).
[20] L. A. Haskin et al. *J. Geophys. Res*. 102, pp. 19293–19306 (1997).
[21] A. Wang et al. *J. Geophys. Res*. 104, pp. 8509–8519 (1999).
[22] J. Ryczkowski, *Catalysis Today,* 124: pp. 11–20 (2007).
[23] M. Touboul et al. *Nature* 450, 1206–1209 (2007).
[24] R. A. Lovett. *Earth-asteroid collision formed moon later than thought.* National Geographic News 2007(12).
[25] A. Brandon. *Nature*. 450. 1169-1170 (2007).
[26] C. Allen and N. S. Todd, *Astromaterials curation - Rocks and soils from the Moon. http://curator.jsc.nasa.gov/lunar/index.cfm*. 2007, NASA.
[27] J. J. Papike et al. *Rev. Geophys. Space Phys*. 14, pp. 475 (1976).
[28] *http://www.nasa.gov/mission¬_pages/apollo/index.html*. NASA National Aeronautics and Space Administration, 2007.
[29] L. R. Gaddis et al., *Icarus,* 161: p. 262 (2003).
[30] E. Dowty, Keil. K., Prinz. *Lunar Planet. Sci*. 5, 174–176 (1974).
[31] J. W. Delano, *Proc. Lunar. Sci.* 6, 15–47 (1975).
[32] D. T. Vaniman, J. J. Papike, E. L. Schweitzer, *Proc. Lunar. Planet. Sci. Conf.* 9, 1827–1860 (1978).
[33] S. B. Simon, J. J. Papike, *Lunar Planet. Sci*. 18, 922–923 (1987).
[34] *Basaltic Volcanism Study Project 1981,* Lunar Planet. Sci. XXXVI: p. 236–267 (2005).
[35] G. E. Snyder, C. R. Neal, L. A. Taylor and A. N. Halliday, *Geochim. Cosmochim. Acta*. 61, 2731–2747 (1997).
[36] M. von Ardenne, *Zeitschrift für Physik,* 108: p. 553–572 (1938).
[37] M. von Ardenne, *Zeitschrift für Technische Physik,* 108: p. 407-416 (1938).
[38] P. Staszczuk, *Thermochimica Acta.* 308: p. 147–147 (1998).
[39] G. Liptay, *Atlas of Thermoanalytic Curves,* 1971–1977, Budapest, London: Akadémiai Kiadó and Heyden.
[40] K. Rübner, E. Robens and D. Balköse, *J. Therm. Anal. Cal.* 2008.
[41] M. Iwan et al. *Analiza termiczna próbek gruntu księżycowego. (Thermal analysis of lunar samples),* in *IX Krajowe Seminarium im. Prof. Stanislawa Bretsznajdera Seminary on Thermal Analysis,* 2007, Instytut Chemii, Politechnika Warszawska, Wydz. Mechaniki i Petrochemii w Plocku: Płock, p. 164–168.

[42] S. Cebulak et al. *J. Therm. Anal. Cal*. 72: p. 405 (2003).
[43] *Crucibles for Thermal Analysis. http://glo.mt.com/mt/resources/productsBrochures.jsp,* 2007. Mettler Toledo.
[44] ISO *ISO 9277: Determination of the specific surface area of solids by gas adsorption using the BET method,* 1995, Berlin: Beuth.
[45] DIN *DIN 66134: Bestimmung der Porengrößenverteilung und der spezifischen Oberfläche mesoporöser Feststoffe durch Stickstoffsorption. Verfahren nach Barrett. Joyner und Halenda (BJH),* 1998, Berlin: Beuth.
[46] S. Brunauer, P. H. Emmett and E. Teller, *J. Am. Chem. Soc*. 60: p. 309 (1938).
[47] E. P. Barrett L. G. Joyner and P. H. Halenda, *J. Am. Chem. Soc.* 73: p. 373–380 (1951).
[48] D. Dollimore, and G. R. Heal, *J. Appl. Chem*. 14: p. 109 (1964).